Blast Shocks in Quasi-Two-Dimensional Supersonic Granular Flows

Jean-François Boudet, J. Cassagne, Hamid Kellay

Blast Shocks in Quasi-Two-Dimensional Supersonic Granular Flows

J. F. Boudet, J. Cassagne, and H. Kellay

Centre de Physique Moléculaire Optique et Hertzienne, Université Bordeaux 1, UMR 5798 CNRS, 351 cours de la Libération, 33405 Talence, France

(Received 10 July 2009; published 25 November 2009)

In a thin, dilute, and fast flowing granular layer, the impact of a small sphere generates a fast growing hole devoid of matter. The growth of this hole is studied in detail, and its dynamics is found to mimic that of blast shocks in gases. This dynamics can be decomposed into two stages: a fast initial stage (the blast) and a slower growth regime whose growth velocity is given by the speed of sound in the medium used. A simple model using ingredients already invoked for the case of blast shocks in gases but including the inelastic nature of collisions between grains accounts accurately for our results. The system studied here allows for a detailed study of the full dynamics of a blast as it relaxes from a strong to a weak shock and later to an acoustic disturbance.

DOI: 10.1103/PhysRevLett.103.224501 PACS numbers: 47.40.Ki, 47.57.Gc

In the 1940s, G. I. Taylor [1] developed simple scaling arguments to account for the consequences of depositing a very large amount of energy in a very small volume and applied them to understand the propagation of a nuclear bomb blast. He backed up his analysis with measurements of the evolution of the radius of the blast versus time from photographs of such explosions. The self similar solutions developed by Taylor [1] and Sedov [2], at about the same time, are known as the Sedov-Taylor blasts [3]. The main prediction of this analysis, which assumes conservation of energy, is that the radius of the blast increases as a power of time with an exponent of $2/5$. This exponent depends on the dimension of space, and in two dimensions, it would be $1/2$ [4]. This prediction has been verified or tested in a number of situations encompassing nuclear bomb blasts [1], laser induced blasts in different gases [4–7], and different transparent materials [8], and is believed to hold for blasts following a supernova albeit with modifications due to radiative losses [9–11]. Numerical simulations even suggest their existence for granular materials [12]. In general, such blasts eventually weaken and transform into an acoustic perturbation traveling at the speed of sound [3,13]. Numerous theoretical, numerical, and experimental studies have been carried out since Taylor's and Sedov's seminal papers to understand such a complex phenomenon under different excitations and different properties of the medium in which the blast occurs [3,11].

Here, by impacting a thin, dilute, and fast flowing granular layer with spheres of different diameters, we observed the expansion of a hole almost devoid of material right after the impact. Analysis of this expansion shows that this phenomenon bears great resemblance to the blast problem. Indeed, the initial stages of the expansion follow a well defined behavior reminiscent of Taylor-Sedov blasts but for the two dimensional case and modified by energy losses due to the inelasticity of the collisions between grains in the granular medium. According to our results, the kinetic energy decreases exponentially with the radius of the shock, and a simple model accounts for most of the features described here. In the late stages, the radius of the blast varies linearly with time, giving an expansion velocity in agreement with the speed of sound in such materials. This late stage is also characterized by a broadening of the shock front, a feature not seen for the early stages of the expansion. This is therefore a simple case for non-energy conserving blasts with a sufficiently slow dynamics so that the experiments explore the full range of the expansion going from the initial stages of the blast up to the latest stages where the disturbance weakens and propagates at the speed of sound.

The experimental setup uses a thin layer of sand flowing on an inclined glass plane (35°, thickness 6 mm). The sand is poured from a funnel shaped container, in the form of a jet as for the previously studied granular jump [14] but on an inclined plane so the flow does not stop because of friction against the solid surface. Near the position of the impact of this jet, the flow is inhomogeneous and divergent over a distance of about 10 cm with a gradient in velocity and density [see Fig. 1(a)]. Beyond this distance, the flow becomes roughly homogeneous over a distance of about 30

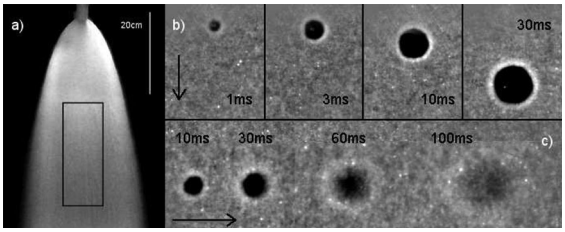

FIG. 1. Images of the expanding hole right after the impact of a steel sphere. (a) An image of the flow produced from a funnel of 2.4 mm in diameter. (b) impact of a 16 mm diameter steel sphere. (c) impact of a 2 mm diameter steel sphere. The hole is surrounded by a dense rim seen here as bright since the images use the backscattered light from the layer. This hole expands fast with a circular rim with a roughly constant width at first but which broadens at later times.

to 40 cm with a lateral width of over 10 cm. This is the region where the experiments are carried out. In this region, the velocity varies by less than 20% over a distance of 20 cm. The flow in this region gives rise to a thin layer of sand, of thickness approximately 1.2 mm, flowing at speeds between 1.2 and 1.7 m/s depending on the distance from the funnel. The velocity of the layer was determined by tracking small inhomogeneities in the flowing layer. The volume fractions used varied between 5% and 20%. This variation was obtained by varying the diameter of the funnel from 1 to 2.5 cm. The produced flow is supersonic with a well defined speed of which was obtained by placing a needle in the flow for which a Mach-like cone is observed [15]. The half angle of this cone gives a speed of sound of 13 ± 2 cm/s independent of the volume fraction and the velocity of the flow for the ranges studied here. Note that other experiments have shown the existence of shock waves and fronts in granular media [16]. The impacting spheres used here are steel spheres of different diameters between 2 and 16 mm which were released vertically from a distance of about 25 cm from the glass plate. The sand used is composed of glass beads of diameter 0.3 mm. The images of the impact were collected from below the glass plate, in order to avoid the spheres, and were recorded with a camera working at rates up to 10 000 frames/second. A diffuse broad white light source was used for illumination in two different configurations where the camera captures either the backscattered light from the particles with dense regions appearing bright or the transmitted light from the stream of particles with dense regions appearing dark. While the intensity of the collected light is not linear versus the density of the layer, it gives information about density variations accurately. In transmission measurements, the collected intensity can be related to the local density of the layer through a monotonic but nonlinear variation as has been shown before [17]. The sequence of images from each impact was then analyzed using a home made computer program.

Figure 1 shows photographs of the impact of the steel spheres on the thin layer of sand. The sphere bounces on the glass surface and does not interfere with the produced hole. The impact does not produce a splash, as confirmed by visualizations from the side, and the density variations are in the plane of the flow. The impacting sphere pushes the sand grains radially outwards from the impact position and produces a small hole in the layer. This hole is seen as dark in these images, as they are taken in the backscattering configuration, and is therefore almost devoid of sand particles shortly after the impact. Notice that this hole is advected by the mean flow and expands rapidly after the impact of the steel sphere. Snap shots of this expansion are shown at different instants of time after the impact for two different sphere diameters. The pattern is characterized by a central region almost devoid of material and a dense outer rim which appears bright in these images. Visualizations from the side indicated that the rim has a height roughly similar to that of the layer. The bottom photographs are for the smaller sphere which gives rise to less dense rims and which we show for longer times after the impact. Note that for the later times, the rim becomes broader and less dense. The inner region also becomes more populated with grains due in part to the broadening of the rim. We have noted that in the very first instants of the impact, the rim is not fully formed but ends up being clearly visible a few tenths of a millisecond after the sphere impacts the layer. Since the layer of sand is of finite thickness, the impacting sphere crosses the sand layer in 0.5 ms before impacting the glass plate. Measurements of the expansion of the rim are started shortly after the impact once the rim becomes clearly distinguishable from the background flow. We quantify the expansion of the resulting hole through two different measurements. The first one locates the position of the rim (through locating its maximum brightness) and gives a measurement of the radius of the pattern versus time after impact. The second one measures the profile of the backscattered or transmitted light intensity (which is a measure of the density of the grains) for different elapsed times. This last measurement is shown in Fig. 2. This color coded map is a spatiotemporal plot of the evolution of the backscattered light intensity profile versus time. The intensity is color coded while the vertical and horizontal axes are the spatial coordinate and the elapsed time, respectively. The maximum of the intensity, or equivalently of the density, travels farther and farther away from the center (impact location). This dynamics is fast at the early instances. At later times, the rim seems to travel at constant speed as indicated by the solid lines in the graph. The width of the profile of the rim increases at the later stages while it remains roughly constant at the early stages.

Figure 3 shows the variation of the radius $R(t)$ of the pattern and the width W of the rim versus time. The individual profiles of the light intensity, obtained in transmission for this plot, are shown in the inset for different times. The transmitted intensity was inverted for these plots in such a way that dense regions have a higher intensity. These profiles show that both the position of the maximum, which we use to define the radius of the hole, and the width of the rim are well defined. Two distinct

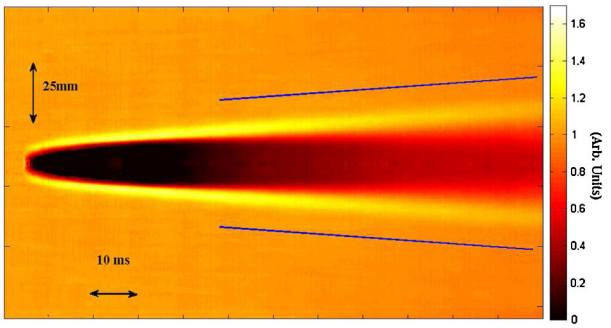

FIG. 2 (color online). Spatiotemporal plot of the angle averaged intensity profile of the hole versus time. This image is color coded in such a way that dense (bright) regions such as the rim appear yellow while less dense regions appear dark.

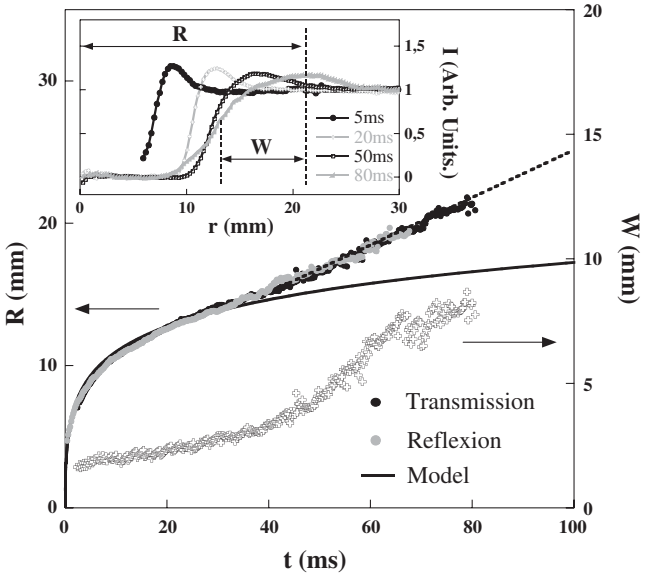

FIG. 3. The radius of the rim R and its width W versus time. Measurements use the backscattered or the transmitted light. The solid line in this graph is a fit to the model proposed in the text while the dashed line indicates propagation at the speed of sound. (diameter of steel sphere = 8 mm, Volume fraction = 0.2). For the fit, $E_0/E_{\text{sphere}} = 10\%$ and $N = 1.67\ \text{mm}^{-1}$. Inset: angle averaged profiles of the rim for different times after impact. The rim profile has a well-defined maximum and has a width which increases with elapsed time.

regimes are clearly seen for the evolution of the radius and the width of the rim. The first fast regime shows a nonlinear variation of the radius versus time while the second regime shows a linear dependence. This linear part is consistent with an expansion at a constant velocity equal to the speed of sound in this material. Basically, this is a circular front propagating at the speed of sound, which was measured independently. The first regime is therefore supersonic and is analogous to the blast shocks discussed in the introduction. For blast shocks in two dimensions, the expansion should follow a well-defined law, that of Taylor with an exponent of $1/2$. However, this law ignores energy dissipation which is common in the collisions of grains. As we will see below, this initial regime can be understood using similar arguments as for blast shocks but accounting for such dissipation. The solid line in this plot is a fit using the model proposed below which fits the nonlinear part very well but deviates from the evolution of the radius when this latter enters a linear propagation regime. The blast weakens with time and enters the acoustic regime at later times [3]. The bottom plot depicts the width of the rim W versus time: W varies slowly in the first regime but increases markedly for the second regime. As time elapses, the density in the rim decreases and its width increases showing the attenuation of this acoustic front at time elapses. For the latest times, the rim becomes barely distinguishable from the background flow as shown in Fig. 1. The evolution of the width of the profile or of the radius did not depend on the lighting mode used and did not depend on the value of the advection speed.

We here propose a simple model to understand the propagation of the blast at its early instants. Let us start by recalling Taylor's prediction for the propagation of such blasts. This argument can be presented dimensionally by noting that if the energy is conserved, the only quantities entering the relation between the radius of the blast R and propagation time t is the deposited energy E and the density of the outer medium ρ_0. This relation, for a three dimensional spherical blast, then reads: $R(t) \sim (E/\rho_0)^{1/5} t^{2/5}$. In two dimensions, the evolution of the radius reads: $R(t) \sim (E/\rho_0 h)^{1/4} t^{1/2}$. Here, we have used $\rho_0 h$ as the two dimensional density of a thin layer of thickness h and density ρ_0. In our case, and because all the particles are ejected from the central region, this relation can be rewritten in the following form: $\frac{1}{2}\rho_0 h \pi R^2(t) V^2(t) = E$, where $V(t)$ is the velocity of the front $dR(t)/dt$ and E is the total kinetic energy. The simplest interpretation of this relation can be worded as follows: the particles contained in a disk of radius R have accumulated at the outer shell of the blast and acquired a velocity V. The total energy of this moving front is fixed by the kinetic energy E released by the impact, $\rho_0 h$ is the two dimensional density of the layer of sand, and $\rho_0 h \pi R^2(t)$ is the total mass of the displaced particles. If E is conserved, we have the two dimensional equivalent of Taylor's relation $R(t) = (\frac{2E_0}{\pi\rho_0 h})^{1/4} t^{1/2}$. However, and since the collisions between grains of mass m are inelastic, a change of the kinetic energy of each particle after each shock has to be accounted for. If r is the inelasticity coefficient of the particle-particle collisions, this loss of kinetic energy for a particle in the rim undergoing a collision with a particle in the outer medium is $\frac{1}{2}(1 - r^2) m V^2(t)$. The total loss due to the interaction between the particles in the moving rim with the surrounding medium can then be written as $dE = -\frac{1}{2}\pi R^2(t)\rho_0 h V^2 (1 - r^2) N dR$. Here, N is the number of collisions per unit length which we assume to be independent of R [12]. The quantity $N dR$ is the number of collisions for each particle in the rim as it travels a distance dR. This relation gives the following expression for the decrease of the kinetic energy as the rim expands: $E = E_0 \exp[-N(1 - r^2)R]$. Only the velocity of the rim is considered since the hole is being advected as a whole by the mean flow of the layer of sand. The use of this expression for the variation of the energy allows us to solve the relation between the radius, the velocity, and the energy to obtain the time of arrival of the rim at a position R. This model gives a good description of our data for the radius versus time as illustrated in Figs. 3 and 4(a). To write this relation in a simple way, we define a rescaled radius $R' = \frac{N}{2}(1 - r^2)R = R/R_0$ and a rescaled time $t' = \frac{1}{4} \times (\frac{2E_0}{\pi\rho_0 h})^{1/2} N^2 (1 - r^2)^2 t = t/t_0$. This relation then reads: $t' = (R' - 1)\exp(R') + 1$. The two relations for the energy and the time of arrival are illustrated in Fig. 4(b). The inset of

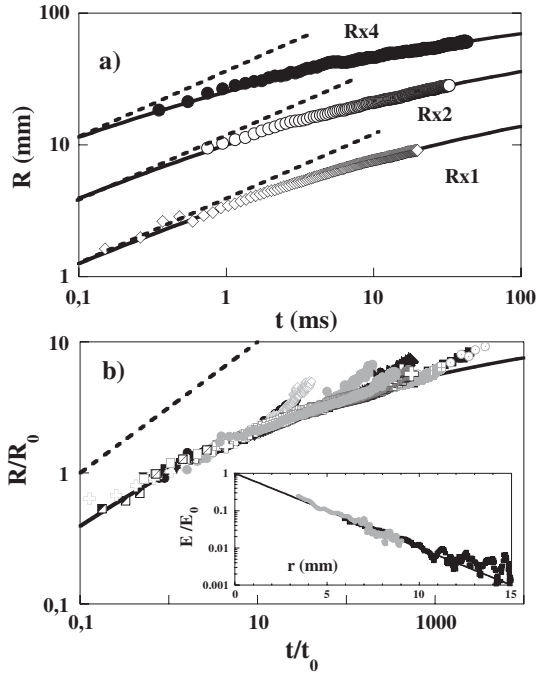

FIG. 4. (a) $R(t)$ along with a fit to the model. Diamonds: steel sphere of diameter 4 mm, volume fraction of 0.2, and the fit parameters are $E_0/E_{\text{sphere}} = 9.4\%$ and $N = 1.6\ \text{mm}^{-1}$. Open circles: steel sphere of diameter 8 mm, volume fraction of 0.2, and the fit parameters are $E_0/E_{\text{sphere}} = 8\%$ and $N = 1.45\ \text{mm}^{-1}$. Closed circles: glass sphere of diameter 16 mm, volume fraction of 0.1, and the fit parameters are $E_0/E_{\text{sphere}} = 20\%$ and $N = 2\ \text{mm}^{-1}$. (b) Collapse of data from different flow volume fractions (from 6 to 22%), different sphere diameters (from 2 to 16 mm), and materials (steel and glass spheres are used). The dashed line is the Taylor-Sedov prediction while the solid line is a fit to our model. The data deviate from the universal regime when the expansion speed approaches the sound velocity. The fit parameters N and E_0/E_{sphere} are between 1.4 and 2.5 mm^{-1} and between 1 and 20%, respectively, for all the runs examined. Inset: E/E_0 versus time. Two sphere diameters (8 and 3 mm) are used. The exponential dependence gives a value of N of 1.67 mm^{-1} and a value of E_0/E_{sphere} of 5 and 10%.

Fig. 4(b) shows that the kinetic energy follows the exponential decrease very well showing that N is a well defined quantity and is independent of time despite the complexity of the interaction of the particles in the rim with the outer medium and with the glass plate. The characteristic energy E_0 turns out to be a small fraction of the energy of the impacting spheres: This energy was typically a few percent of the kinetic energy of the impacting sphere E_{sphere} and varied from 1 to 20%. The value of $\frac{1}{2}N(1 - r^2)$ varied between 0.2 and 0.35 mm^{-1} for the different runs we have examined giving a value for N between 1.4 and 2.5 mm^{-1} ($r = 0.85$ for glass beads [17]). No systematic dependence on the diameter of the impacting sphere nor on the density of the flow, to within experimental uncertainties, was found. The value of N turns out to be different but comparable in order of magnitude to the inverse mean free path in the outer layer which varies between 1.4 and 6 mm^{-1}. It is possible that the collisions with the bottom plate as well as the three dimensional nature of the rim, effects difficult to include in our simple model, play a role in fixing the value of N. While individual expansion curves can be fit, using our model, as shown in Fig. 4(a), Fig. 4(b) shows that expansion data from different radii of impacting spheres and different densities for the flowing layer can be collapsed on a single master curve as predicted by the model. Note that the model prediction asymptotes to the quoted Taylor-Sedov relation, the dashed line in the graph with a slope of $1/2$, for a two dimensional medium, but our data remain far from this asymptotic regime. The late time regime does not collapse on this curve, and as we have specified earlier, the velocity in this regime is constant and is that of the speed of sound.

In conclusion, thin flowing sand layers have been used to generate quasi-two-dimensional granular blasts whose main properties can be understood using a simple model. A key ingredient of our proposed model is that the energy decreases during the expansion of the blast due to inelastic particle collisions. This allows for an analytic expression of the expansion of the radius of the blast versus time which is borne out experimentally. Our system is therefore a model for nonenergy conserving blasts which are important for different processes in astrophysics, the interaction of intense lasers with different materials, and for blasts in general.

We would like to thank Y. Amarouchene for discussions.

[1] G. Taylor, Proc. R. Soc. A **201**, 159 (1950); **201**, 175 (1950).
[2] L. I. Sedov, J. Appl. Math. Mech. **10**, 241 (1946).
[3] Ya. B. Zel'dovich and Yu. P. Raizer, *Physics of Shock Waves and High Temperature Hydrodynamic Phenomena* (Dover Publications, Inc., New York, 2002).
[4] J. F. Kielkopf, Phys. Rev. E **52**, 2013 (1995).
[5] J. Grun *et al.*, Phys. Rev. Lett. **66**, 2738 (1991).
[6] M. J. Edwards *et al.*, Phys. Rev. Lett. **87**, 085004 (2001).
[7] A. D. Edens *et al.*, Phys. Plasmas **11**, 4968 (2004).
[8] E. G. Gamaly *et al.*, Phys. Rev. B **73**, 214101 (2006).
[9] E. Cohen, T. Piran, and R. Sari, Astrophys. J. **509**, 717 (1998).
[10] E. Lian and K. Keilty, Astrophys. J. **533**, 890 (2000).
[11] J. P. Ostriker and C. F. McKee, Rev. Mod. Phys. **60**, 1 (1988).
[12] T. Antal, P. L. Krapivsky, and S. Redner, Phys. Rev. E **78**, 030301 (2008).
[13] H. Steiner and W. Gretler, Phys. Fluids **6**, 2154 (1994).
[14] J. F. Boudet *et al.*, J. Fluid Mech. **572**, 413 (2007).
[15] Y. Amarouchene and H. Kellay, Phys. Fluids **18**, 031707 (2006).
[16] E. C. Rericha *et al.* Phys. Rev. Lett. **88**, 014302 (2001); J. Bougie *et al.*, Phys. Rev. E **66**, 051301 (2002).
[17] J. F. Boudet, Y. Amarouchene, and H. Kellay, Phys. Rev. Lett. **101**, 254503 (2008).